*Presented at the 32nd European PV Solar Energy Conference and Exhibition, 20-24 Juni 2016, München, Germany*

# ALTERNATIVE INLINE ANALYSIS OF ACIDIC ETCHING BATHS

L. Mohr, T. Dannenberg, M. Zimmer, J. Rentsch
Fraunhofer Institute for Solar Energy Systems ISE
Heidenhofstraße 2, 79110 Freiburg, Germany
Phone: +49 761 4588 5657. E-Mail: lena.mohr@ise.fraunhofer.de

ABSTRACT: A process control system was developed which continuously monitors the composition of acidic etching baths. The simple physical parameters, sound velocity, conductivity, and refractive index are verified for suitability to determine the concentrations of hydrofluoric acid, nitric acid, and hexafluorosilicic acid. In pre-tests the characteristics of the individual concentrations were observed with the measuring devices and the effect of the formation of nitrous gases on the physical measuring devices is observed. In contrast to the conductivity electrode, the sound velocity and refractive index sensors show highly reproducible results. The formation of nitrous gases has no significant effect on the physical measurement methods. The influence of different concentrations of a mixture on the physical parameters is determined building up a design of experiment. With aid of multiple linear regression model equations were created which describe the quantitative relationship between the concentration and the physical variables. The model equations which lead to a quantitative correlation between the concentration of the acids as a function of the parameters sound velocity, conductivity, refractive index and temperature are compared and finally validated. The model equation predicts the concentration of HF with a recovery rate of 96.40%, $HNO_3$ with 96.38% and Si in $H_2SiF_6$ with 78.74%.
Keywords: Silicon Solar Cells, Manufacturing and Processing, Etching, Design of Experiments, Modelling

## 1 INTRODUCTION

Acidic based etching baths are frequently used for industrially manufacturing of multicrystalline silicon solar cells, mainly for texturization and rear side polishing before diffusion [1,2]. The resulting surface morphology after etching particularly relies on the composition of the solution, consisting of hydrofluoric acid (HF) and nitric acid ($HNO_3$) [3,4]. During the processes different reaction products are formed, especially hexafluorosilicic acid ($H_2SiF_6$) and the concentrations of the reactants decrease. This means that monitoring of the composition is indispensable, to achieve stable process results. Currently, analytical methods such as titration, near infrared spectroscopy (NIRS) and ion chromatography (IC) with post column derivatization and UV-Vis detection for determination of solved silicon, are used [5–7]. These methods have been successfully implemented but the analysis instruments have high costs of ownership and trained manpower is required. Inline analytics allow, unlike the offline and atline processes, a continuous correlation between the obtained information and the properties of the process [8]. Inline monitoring is commonly used for classical measured variables, such as temperature, pressure or flow. However, further research is needed in the process control of mixtures and their compositions [9]. Due to calibration relationships a concentration can be determined by means of physical dimensions (as electrical, acoustical or optical values). For example, ultrasonic measurement is gaining more and more importance, because it provides a reproducible, non-invasive measurement of flow rate and in some cases concentration, with short time response [8]. However, other measuring devices have similar advantages and in a mixture of components, more variables are needed, such as refractive index ($n$) or conductivity ($\kappa$) which can be linked to the ultrasonic velocity ($c$). The reference methods used were titration as well as ion chromatography.

## 2 EXPERIMENTAL

### 2.1 Preliminary tests

A series of measurements of each acid – HF, $HNO_3$, $H_2SiF_6$ - was taken with the physical devices to observe the physical behavior change within the different concentrations and to gain knowledge about the handling and the operating range. In addition two measuring points of each curve were taken on different days in order to check the reproducibility of the analytical equipment. Furthermore a mixture (reference solution) of $c_{HF}$ = 60 g/l, $c_{HNO_3}$ = 600 g/l and $c_{Si\ in\ H_2SiF_6}$ = 5 g/l was prepared to perform long-term measurements. This mixture was in the range of the composition of a polishing bath.

### 2.2 $NO_x$ test

During texturing nitrogen oxides are formed which lead to a yellowing of the solution due to the reaction with $HNO_3$ and Air [10,11]. To rule out interference on the measuring devices due to this reaction, a $NO_x$ experiment was built up. Various solutions of different acid concentrations ($HNO_3$, HF, $H_2SiF_6$) and the reference solution were produced and their exact concentrations recorded using the reference methods. Furthermore, the physical parameter of the test solutions and a blank value were recorded before the $NO_x$ experiment was carried out. Nitrogen dioxide ($NO_2$) was produced in a reaction chamber, filled with 10% $HNO_3$ and a diluted sodium nitrite solution ($NaNO_2$), according to equation (1), so that a strong yellow coloration was achieved.

$$2\ NaNO_2(l) + 2\ HNO_3(l) \rightarrow 2\ NaNO_3(l) + NO_2(g) + NO(g) + H_2O(l) \quad (1)$$

The $NO_2$ is passed through a gas washing bottle filled with solution, thereby turning it yellow. Immediately, the solutions were measured again with the physical devices and the reference method.

### 2.3 Design of Experiments (DoE)

The influence of the different concentrations of a

mixture on the physical parameters was determined building up a Design of Experiments (DoE). An orthogonal and rotatable central composite design (CCD) was created, with the response values $n$, $\kappa$ as well as $c$ and the factors HF, $HNO_3$, $H_2SiF_6$ and temperature ($t$). The factor levels were: $c_{HF}$ (g/l) = {50, 70}, $c_{HNO3}$ (g/l) = {500, 700}, $c_{Si\ in\ H2SiF6}$ (g/l) = {0.5, 9.5} and $t$ (°C) = {10, 30}. To draw conclusions about the amount of Si which is brought in during the process basin the factor $H_2SiF_6$ is given as Si in $H_2SiF_6$. The experimental design, consisting of 36 solutions, was randomized and measured in an experimental setup (fig. 1). The conductivity sensor was placed in the solution. The solution was circulated through a temperature basin to achieve specific temperatures, followed by the refractometer and sound velocity sensor.

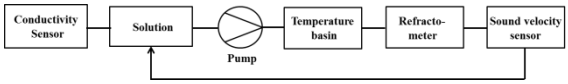


**Figure 1:** Flow diagram of the experimental design setup

The aim was to obtain an empirical model, which quantitatively describes the relationship between the studied factors (concentration of the acids) and the response values (physical variables). With the aid of multiple regression, model equations were created [12]. A general regression model with $k = 4$ factors based on a linear combination of basic functions, was used.

$$y_i = \beta_0 + \sum_{i=1}^{k} \beta_i x_i + \sum_{i=1}^{k} \beta_{ii} {x_i}^2 + \sum_{i=1}^{k} \sum_{j=i+1}^{k} \beta_{ij} x_i x_j \qquad (2)$$

With the response value (dependent variable) $y_i$, the regression coefficients $\beta_i$ and linear $x_i$, squared $x_i^2$ as well as interactive $x_i x_j$ effects (explanatory or independent value). The modeling was done by progressive elimination of factors and interactions which did not show a significant effect on the response value. The analysis of variance (ANOVA) has been used to investigate the significance of true effects. ANOVA uses variance estimates to compare response mean differences [13]. The variance of response values is explained by the influence of various factors. In order to assess if the factors have a significant impact on the acid concentration, the coefficients are compared with the width of the confidence interval. The beta coefficients ($Beta_j$), in contrast to the regression coefficients ($\beta_i$) allow the comparison with each other. Due to the different units within the regression coefficients it is not possible to get information about the strength of changing on the response value by marginal changes of the coefficients. Standardized beta coefficients

$$Beta_j = \beta_j \frac{s_{xj}}{s_y} \qquad (3)$$

allow a relative comparison of the explanatory values [14], with the standard deviation $s_{xj}$ of the independent variable $x_j$ and the standard deviation of the dependent variable $s_y$. Thus, the $Beta_j$ indicates the change in the response value with a change of the independent variables by one standard deviation (of $x_j$) while keeping all other independent variables constant. During the evaluation high beta values could indicate multicollinearity. This occurs, if there is a linear relationship between two or more independent variables. This problem of regression analysis may affect the accuracy of the model equation. A relatively simple identification is the variance inflation factor (*VIF*).

$$VIF_j = \frac{1}{1 - R_j^2} \qquad (4)$$

Where $R_j^2$ is the coefficient of determination obtained by regressing the $j^{th}$ independent variable on the remaining independent variables. A *VIF* of 1 corresponds to the ideal state, a $VIF \geq 10$ indicated already a high multiple correlation [15]. For the model validation a confirmatory test run was carried out. Six different solutions were prepared and detected with the experimental setup. The solutions contain random compositions of acids in the concentration range of the experimental design.

## 3 RESULTS AND DISCUSSION

### 3.1 Preliminary tests

In order to identify trends, two solutions at each concentration series were analyzed repeatedly at different days. Sound velocity and conductivity were taken tenfold, refractive index threefold and the reference solution 16-fold. The reproducibility of the sensoric devices was expressed via the relative standard deviation ($\upsilon$) and is listed for each repeated measurement as well as for the reference solution in table I. Figure 2 (i) shows the results of the preliminary tests sound velocity as a function of weight percent for different acids. A good reproducibly, which can be seen on the replicate points and the υ results of the reference solution (table 1) was observed. The curve of HF in contrast to the other acids decreases with increasing concentration. To explain this curve progression, equation (5) was used and the bulk modulus plotted as a function of weight percent [16].

$$c^2 = \frac{1}{\rho \cdot \delta} \qquad (5)$$

With sound velocity $c$, density ρ and the bulk modulus $\delta$. Figure 3 (ii) shows that the bulk modulus of $\delta_{H2SiF6}$ decreases with a greater gradient than $\delta_{HF}$ ($\delta_{H2SiF6} > \delta_{HNO3} > \delta_{HF}$). In addition, the density is plotted against the concentration in weight percent (fig. 2 (iii)). The results show that the bulk modulus of $H_2SiF_6$ in contrast to the HF falls steeply, thus the denominator in equation (5) becomes smaller, whereby the sound velocity becomes larger. The bulk modulus of HF changes only slightly with increasing concentration. This means that the density of HF has the greater influence in equation (5), the denominator becomes larger and the sound velocity decreases. It should be noted that the non-linearity of the $HNO_3$ for high concentrations occurs in the standard measuring range which may lead to misinterpretations during the equation modeling (fig. 2 (i)).

**Table I:** Mean relative standard deviation ($\upsilon$) for the replicates and the reference solution.

| Relative Standard deviation | $c$ [%] | $\kappa$ [%] | $n$ [%] |
|---|---|---|---|
| $HNO_3$ | 0.06 | 13.64 | 0.11 |
| HF | 0.05 | 10.67 | 0.004 |
| Si in $H_2SiF_6$ | 0.09 | 9.64 | 0.01 |
| Reference solution | 0.14 | 1.97 | 0.03 |

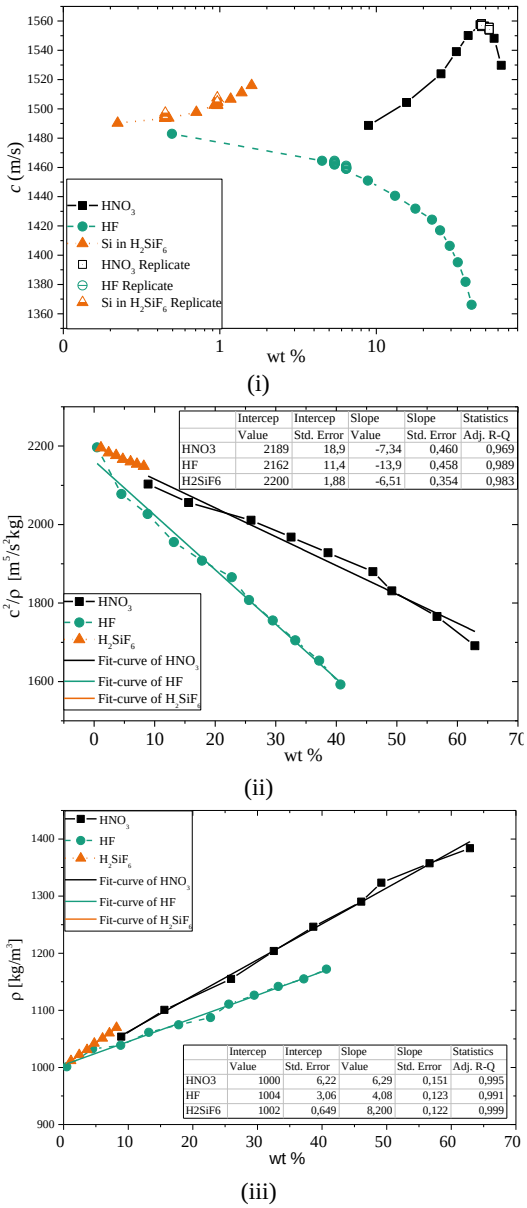


**Figure 2:** Sound velocity (i), bulk modulus (ii) and density (iii) of individual acids as a function of the concentration in weight percent.

Figure 3 (i) shows the difference between strong and weak electrolytes. Strong electrolytes, such as $HNO_3$ differ in high concentrations due to the relaxation and electrophoretic effects from linear behavior. The $HNO_3$ curve reaches up to a conductivity of almost 900 mS/cm. It should be noted that the non-linearity of the $HNO_3$ curve could lead to misinterpretation during the equation modeling. Furthermore the conductivity electrode shows in this region a high relative standard deviation (table 1). In comparison, the standard deviation of the standard solution shows a low value of 1.97%. This is due to the lower conductivity of the standard solution and the associated proximity to the calibration range. The reproducibility of the refractometer is very good, as demonstrated by the low relative standard deviations in table 1 column *n* and the replicate points on the curve in figure 3 (ii).

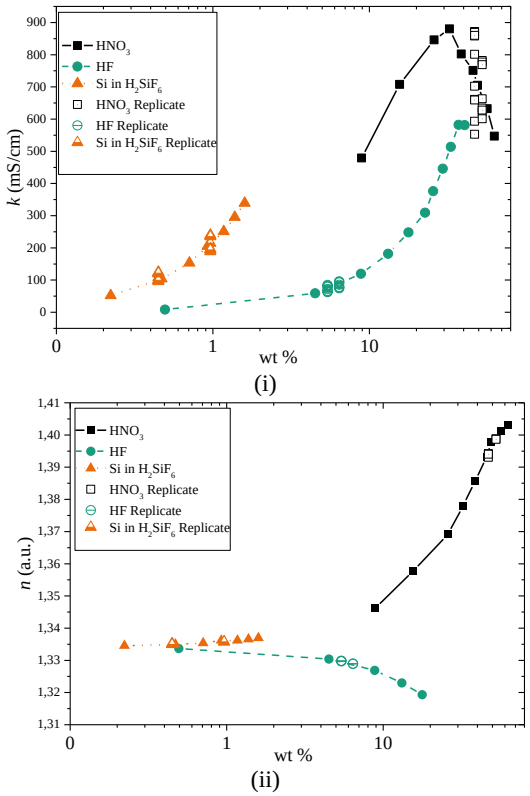


**Figure 3:** Conductivity (i) and refractive index (ii) of individual acids as a function of the concentration in weight percent.

### 3.2 $NO_x$ test

To examine the effect of the nitrous gases the relative standard deviation is estimated with the values of the physical measurement devices before and after the experiment as well as with ion chromatography. The results of the ion chromatography show that during the experiment $NO_2$ has increased with an average of $m_{NO2}$ = 345.2 mg. The mean relative standard deviation of all samples per each physical device was calculated. The highest value was found for the conductivity sensor $\upsilon_\kappa$ = 1.581%, the least for the refractometer $\upsilon_n$ = 0.003%. The mean relative standard deviation of the sound velocity was $\upsilon_c$ = 0.009%. Despite a low increase in the amount of nitrite no or negligible effects on the physical measurement methods are expected during a HF-$HNO_3$ process.

### 3.3 DoE

For the statistical evaluation, especially the modelling the factors and response values of the CCD are exchanged to obtain an empirical model, which quantitatively describes the relationship between the concentration of the acids ($c_{HF}$, $c_{HNO3}$, $c_{Si\ in\ H2SiF6}$) and the physical variables (*n*, *κ*, *c*, *t*). The following pareto charts (fig. 5) of standardized (*Beta*) coefficients show the significant variables of the respective response value out of all effects (eq. (2)). During the evaluation the significance level (p-value) was set to 0.05 which means that the results are representative with a 95% level of confidence. Due to the use of beta coefficients information is obtained how a change of a factor affects the response value. These factors are listed in figure 4 in descending magnitude.

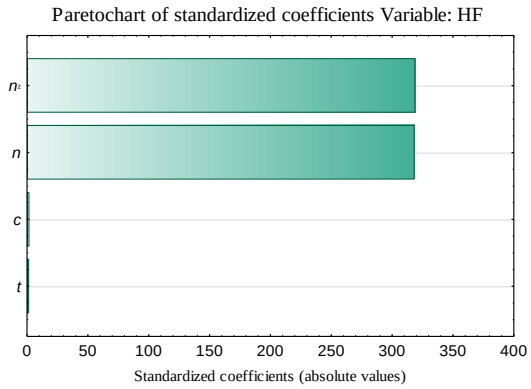


(i)

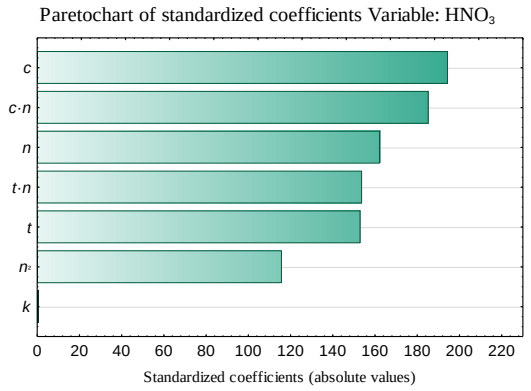


(ii)

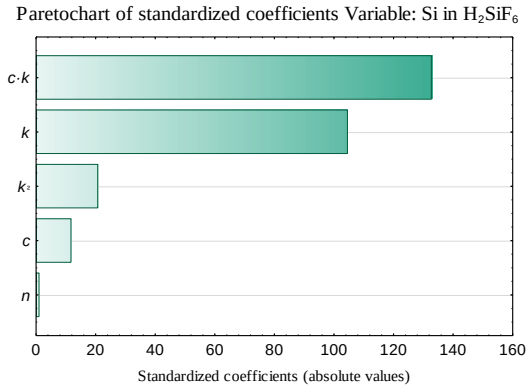


(iii)

**Figure 4:** Pareto charts of standardized coefficients of the response values HF (i), $HNO_3$ (ii) and Si in $H_2SiF_6$ (iii).

The concentration of HF is determined with the use of the physical devices refractive index, sound velocity and the aid of temperature as shown in figure 4 (i). A change in refractive index value – squared ($n^2$) and linear ($n$) - has the greatest impact on the concentration of HF. A small change in sound velocity and in the interaction of sound velocity with refractive index indicates a big change in the concentration of $HNO_3$ (fig. 4 (ii)). Compared to HF (four terms) the equation of $HNO_3$ involves more terms (seven terms), including linear ($c$, $n$, $t$, $\kappa$), interactive ($c{\cdot}n$, $t{\cdot}n$) and a squared term ($n^2$). To determine the concentration of Si in $H_2SiF_6$ five terms are needed, including the linear values of $\kappa$, $c$ and $n$ the interaction of $c$ and $\kappa$ and $\kappa^2$ (fig. 4 (iii)). With these pareto charts it is shown, that a change in refractive index mainly indicates a change in the concentration of HF, a change in sound velocity mainly indicates a change in $HNO_3$ and a small change in the conductivity mainly indicates a big change in Si in $H_2SiF_6$. The presumption of multicollinearity, indicated by very high beta values was confirmed by calculating the *VIF* (table II). It was found that in the linear terms of the equation the temperature ($VIF_t \approx 5$) correlates with the physical variables. Moderate correlation is not necessarily problematic; the variance of the regression coefficient increases, which could lead to a less accurate prediction of acid concentrations. The tolerance in table II is defined as $1\text{-}R^2$. The smaller a tolerance of a variable, the redundant is their contribution to the regression.

**Table II:** *VIF* of the linear factors $c$, $n$, $t$, $\kappa$.

| | Tolerance | *VIF* | $R^2$ |
|---|---|---|---|
| $t$ | 0.1973 | 5.07 | 0.8027 |
| $c$ | 0.2210 | 4.52 | 0.7790 |
| $\kappa$ | 0.2607 | 3.84 | 0.7393 |
| $n$ | 0.3793 | 2.64 | 0.6207 |

The results graphically shown in the pareto charts can also be described as model equations:

$$y_{HF} = \beta_1 + \beta_{1,1}x_c + \beta_{1,3}x_n + \beta_{1,4}x_t + \beta_{1,3}{x_n}^2 \quad (6)$$

$$y_{HNO_3} = \beta_2 + \beta_{2,1}x_c + \beta_{2,2}x_\kappa + \beta_{2,3}x_n + \beta_{2,4}x_t + \beta_{2,5}x_c x_n + \beta_{2,6}x_t x_n + \beta_{2,8}{x_n}^2 \quad (7)$$

$$y_{Si\ in\ H_2SiF_6} = \beta_3 + \beta_{3,1}x_c + \beta_{3,2}x_\kappa + \beta_{3,3}x_n + \beta_{3,7}x_c x_\kappa + \beta_{3,9}{x_\kappa}^2 \quad (8)$$

With $\beta_{ij}$ where i = {HF, $HNO_3$, Si in $H_2SiF_6$} and j = {$c$, $\kappa$, $n$, $t$, $c{\cdot}n$, $t{\cdot}n$, $c{\cdot}\kappa$, $n^2$, $\kappa^2$}. The adequacy of the model equation is expressed by the adjusted coefficient of determination. The value $y_{HNO3}$ with $R^2_{ad} = 0.9737$ is close to 1 and indicates a true description of the actual concentrations with the model. The results of $y_{HF}$ ($R^2_{ad} = 0.5045$) and $y_{Si\ in\ H2SiF6}$ ($R^2_{ad} = 0.4157$) are very low. In figure 5 (i), (ii) and (iii) the observed versus the predicted values of each acid are shown. Especially in figure 5 (i) and (iii) the distribution of the predicted values is high, which reflects the low $R^2_{ad}$ values of HF and Si in $H_2SiF_6$. Especially the moderate adjusted coefficient of determination of Si in $H_2SiF_6$ could be caused by the high relative standard deviation of the conductivity, since this value is present in equation (8) in three out of five effects. That the observed values do not scatter, is due to the consistent concentrations of the acids, which have been used for the DoE.

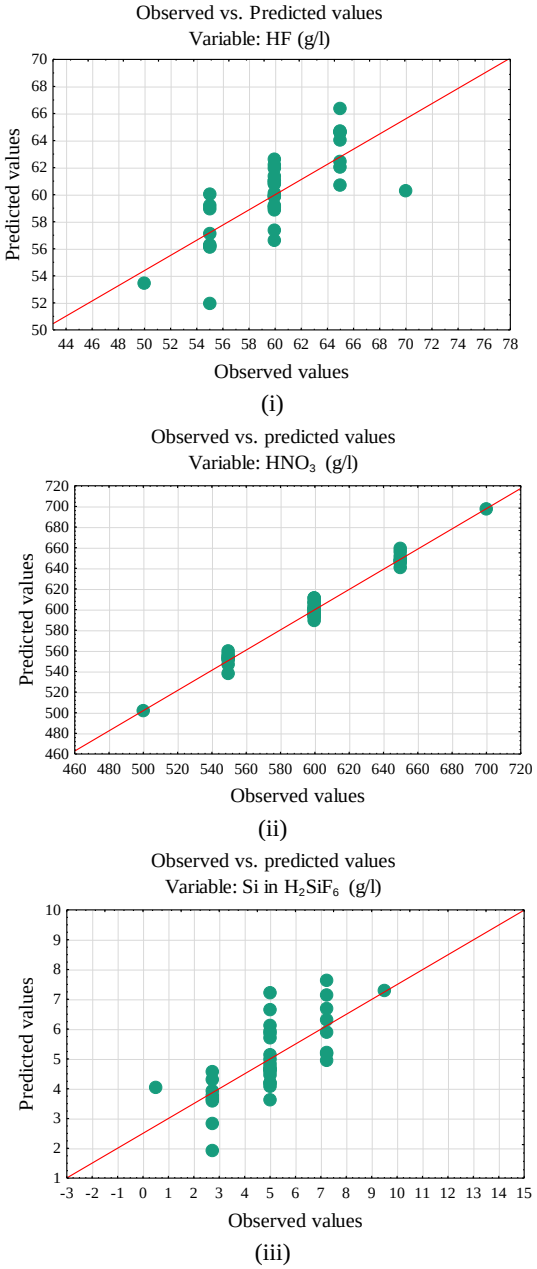


**Figure 5:** Observed versus predicted values and the adjusted determination of coefficient of the response value HF (i), $HNO_3$ (ii) and Si in $H_2SiF_6$ (iii).

### 3.4 Validation

The model equations have been validated with a test run. Therefore six solutions with different concentrations of $HF/HNO_3/Si$ in $H_2SiF_6$ have been used. The values of $c$, $n$, $t$, $\kappa$ were obtained and the intermediate recovery rate calculated. Although model $y_{HF}$ shows a less $R^2_{ad}$ the result of the intermediate recovery rate is the highest with 96.40%. The concentration of $HNO_3$ was found with an accuracy of 96.38%. The model equation for Si in $H_2SiF_6$ with an accuracy of 78.74% leads to a big uncertainty of results. The model equations are valid for the concentration range seen in figure 5 and should not be extrapolated.

## 4 SUMMARY

This work demonstrates as proof of concept that through the combination of sound velocity, conductivity and refractive index a system can be developed, which can be used for the inline analysis of all main components of etching baths. In preliminary tests was shown that the measuring results of sound velocity and refractive index are very reproducible compared to conductivity. In addition it was observed that $NO_x$ gases have no or negligible effects on the physical devices. The influence of different acid concentrations with respect to the physical parameters could be determined using DoE. With the aid of multiple linear regression model equations were created which describe the relationship between the concentration of HF, $HNO_3$ and Si in $H_2SiF_6$ and the physical values $c$, $n$, $t$, $\kappa$. The concentration range used were HF 50 - 70 g/l, $HNO_3$ 500 - 700 g/l and Si in $H_2SiF_6$ 0.5 - 9.5 g/l. The measuring temperature should be between 10 and 30 °C. Furthermore it should be noted that the presumption of multicollinearity indicated by high beta-values was confirmed. The model equation predicts the concentration of HF with a recovery rate of 96.40%, $HNO_3$ with 96.38% and Si in $H_2SiF_6$ with 78.74%.

## 5 ACKNOWLEDGEMENTS

This work was funded by the German Federal Ministry for the Environment, Nature Conservation and Nuclear Safety under the frame of the project “NAPOLI” (0325654B).

## 6 REFERENCES

[1] D.-H. Neuhaus, A. Münzer, "Industrial Silicon Wafer Solar Cells", *Advances in OptoElectronics*, 2007.

[2] X. Liu *et al.*, "Black silicon: fabrication methods, properties and solar energy applications", *Energy & Environmental Science*, vol. 7, no. 10, pp. 3223–3263, 2014.

[3] H. Robbins, B. Schwartz, "Chemical Etching of Silicon", *J. Electrochem. Soc.*, vol. 106, no. 6, p. 505, 1959.

[4] H. Robbins, B. Schwartz, "Chemical Etching of Silicon", *Journal of The Electrochemical Society*, vol. 107, p. 108, 1960.

[5] M. Zimmer, A. Oltersdorf, J. Rentsch, "Online process control of acidic texturisation baths with ion chromatography", *Talanta*, vol. 80, no. 2, pp. 499–503, 2009.

[6] A. Henßge, J. Acker, "Chemical analysis of acidic silicon etch solutions: I. Titrimetric determination of HNO, HF, and H SiF", *Talanta*, vol. 73, no. 2, pp. 220–226, 2007.

[7] M. Zimmer *et al.*, "Towards the automation of the acidic texturisation process", *European Commission: 25th European Photovoltaic Solar Energy Conference and Exhibition, EU PVSEC 2010. Proceedings: 5th World Conference on Photovoltaic Energy Conversion, 6-10, September 2010, Valencia, Spain. München: WIP-Renewable Energies, 2010, pp. 1719-1721*, 2010.

[8] Kessler, Rudolf W., "Prozessanalytik", WILEY-VCH Verlag GmbH & Co. KGaA, 2006.
[9] J. Sacher, Rg, "Ein Ohr für PAT", *Chemie Technik, Heidelberg*, vol. 36, no. 7, pp. 72–74, 2007.
[10] K. Mayer, "Chemische Ansätze zur Neuordnung des Solarzellenprozesses ausgehend vom Wafering bis hin zur Emitterdiffusion, 2009.
[11] Kästner, Gero, "Gas phase characterization of acidic etching mixtures for industrial single side solar cell prodction sequences, Master Thesis, 2013.
[12] A. González, "Two level factorial experimental designs based on multiple linear regression models", *Analytica Chimica Acta*, vol. 360, no. 1-3, pp. 227–241, 1998.
[13] Allen, Theodore T., "Introduction to Engineering Statistics and Lean Sigma: Statistical Quality Control and Design of Experiments and Systems", Springer London, 2010.
[14] Ernst, Huib, "Angewandte Statistik in Geografie und Umweltwissenschaften", vdf Hochschulverlag AG an der ETH Zürich, 2011.
[15] F. Y. HSIEH *et al.*, "An Overview of Variance Inflation Factors for Sample-Size Calculation", *Evaluation & the Health Professions*, vol. 26, no. 3, pp. 239–257, 2003.
[16] U. Hempel, S. Wöckel, J. Auge, "Ultraschallbasierte Informationsgewinnung in der Verfahrenstechnik", *Chemie Ingenieur Technik*, vol. 82, no. 4, pp. 491–502, 2010.